Contents lists available at ScienceDirect

Spectrochimica Acta Part A: Molecular and Biomolecular Spectroscopy

journal homepage: www.elsevier.com

Multianalytical non-invasive characterization of phthalocyanine acrylic paints through spectroscopic and non-linear optical techniques

Alice Dal Fovo [a, b, *], Mohamed Oujja [c], Mikel Sanz [c], Alejandro Martínez-Hernández [c], Maria Vega Cañamares [d], Marta Castillejo [c], Raffaella Fontana [a]

[a] Consiglio Nazionale delle Ricerche - Istituto Nazionale di Ottica, CNR-INO, Largo Enrico Fermi 6, 50125 Firenze, Italy
[b] Università degli Studi di Firenze, Dip. Chimica, Via della Lastruccia 3, 50019 Sesto Fiorentino, Firenze, Italy
[c] Instituto de Química Física Rocasolano, CSIC, Serrano 119, 28006 Madrid, Spain
[d] Instituto de Estructura de la Materia, CSIC, Serrano 121, 28006 Madrid, Spain

ARTICLE INFO

Article history:
Received 27 June 2018
Received in revised form 10 September 2018
Accepted 21 September 2018
Available online xxx

Keywords:
Spectroscopic techniques
Non-invasive analysis
Phthalocyanine paints
Non-linear optical microscopy
Multi-photon excitation fluorescence
Optical coherence tomography
Stratigraphy

ABSTRACT

The documentation and monitoring of cleaning operations on paintings benefit from the identification and determination of thickness of the materials to be selectively removed. Since in artworks diagnosis the preservation of the object's integrity is a priority, the application of non-invasive techniques is commonly preferred. In this work, we present the results obtained with a set of non-invasive optical techniques for the chemical and physical characterization of six copper-phthalocyanine (Cu-Pc) acrylic paints. Cu-Pc pigments have been extensively used by artists over the past century, thanks to their properties and low cost of manufacture. They can also be found in historical paintings in the form of overpaints/retouchings, providing evidence of recent conservation treatments. The optical behaviour and the chemical composition of Cu-Pc paints were investigated through a multi-analytical approach involving micro-Raman spectroscopy, Fibre Optics Reflectance Spectroscopy (FORS) and Laser Induced Fluorescence (LIF), enabling the differentiation among pigments and highlighting discrepancies with the composition declared by the manufacturer. The applicability of Non Linear Optical Microscopy (NLOM) for the evaluation of paint layer thickness was assessed using the modality of Multi-photon Excitation Fluorescence (MPEF). Thickness values measured with MPEF were compared with those retrieved through Optical Coherence Tomography (OCT), showing significant consistency and paving the way for further non-linear stratigraphic investigations on painting materials.

1. Introduction

Today azo and polycyclic compounds, including phthalocyanine, perylene, diaxozine, DPP (diketopyrrolo-pyrrole), indanthrene and quinacridone, are among the most important synthetic organic pigments in the worldwide production [1]. Linstead [2,3] was the first to define the molecular structure of phthalocyanine in 1933, whose name derives from the phthalic acid derivatives used for the pigments synthesis and from the greenish-blue of their hue (cyan from the Greek κυανος). Phthalocyanine (Pc) molecule consists of four isoindole units (C_8H_7N) connected by four nitrogen atoms forming a macrocycle. Copper phthalocyanines (Cu-Pc) are metal complexes where a Cu^{2+} cation occupies the central cavity of the macrocycle and forms covalent bonds with the N atoms (Fig. 1). Cu-Pc α-, β-, and γ- polymorphic forms are widely used as blue and green pigments, referenced as PB15 and PG7 (class 74) in the Colour Index Database (Society of Dyers and Colourists and American Association of Textile Chemists and Colorists) [4]. Various artists, inter alia Magritte, Picasso, Lichtenstein, Mondriaan, Kandinsky and Pollock, made use of PB15 pigments between 1935 and 1990 [5–8].

Phthalocyanine paints owe their success to their remarkable properties, such as ease of use, low cost of manufacture, excellent lightfastness, heat stability up to 550 °C and good resistance to most solvents [9]. The partial solubility of Cu-Pc in aromatic solvents, though, may lead to colour changes (blue towards green) due to crystallization defects occurring during the transition from α- to β- polymorphic form with concurrent growth in crystals size [10]. Since aromatic compounds, especially toluene and xylene, are used as solvent agents in several varnishes and adhesives for paintings, the risk of deterioration of Cu-Pc pigments is significantly high. To prevent damages, it is crucial to identify the presence of Cu-Pc before any restoration treatment involving the removal or application of protective agents/consolidants. Modern pigments, like Cu-Pc, can be found in historical paintings in the form of pictorial retouchings, especially when the original colours were toxic or unavailable [6]. Therefore, the detection of Cu-Pc overpaints may provide evidence of previous conservation treatments. Generally, when a foreign superficial material infringes the ethical standards of restoration – i.e. a pictorial re-

* Corresponding author at: Consiglio Nazionale delle Ricerche - Istituto Nazionale di Ottica, CNR-INO, Largo Enrico Fermi 6, 50125 Firenze, Italy.
Email address: alice.dalfovo@ino.it (A.D. Fovo)

https://doi.org/10.1016/j.saa.2018.09.040
1386-1425/

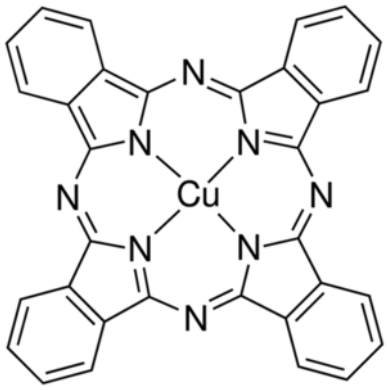

Fig. 1. Copper phthalocyanine molecule. A Cu^{2+} cation occupies the central cavity of the macrocycle forming covalent bonds with N.

touching overlapping the historical paint or being excessively recognizable in terms of colour difference – or does not fulfil its protective/aesthetic function anymore, it has to be thinned down or selectively removed. The cleaning process is an irreversible and delicate intervention, which may greatly benefit from the precise identification of the unwanted layer, as well as the estimation of its extension in-depth. In this sense, it is important to chemically and physically characterize the constituting materials before, during and after any restoring operation, both for documentation and monitoring purposes. Since in cultural heritage diagnosis the preservation of the artwork's integrity is a priority, in-situ, non-invasive modalities, namely not involving sampling, pre-treatments or movements of the object, are generally preferred.

Among the various non-invasive spectroscopic techniques, Raman spectroscopy, Vis-NIR Fibre Optics Reflectance Spectroscopy (FORS), and Laser Induced Fluorescence (LIF) are well-established and widely used for the study of the chemical composition of paint materials. Raman spectroscopy [11] allows for the assignment of the molecular composition according to the vibrational frequencies of chemical bonds present in both inorganic and organic compounds. Vis-NIR FORS is used to probe pigments and identify molecular functional groups, i.e. absorption bands due to overtones and combinations of fundamental vibrations [12]. When applied in combination with Raman spectroscopy, FORS facilitates the identification of chemical compounds, especially when the detection of the Raman signal is hampered by the intense fluorescence emitted by binders and varnishes [13], or when different pigments show similar Raman spectra (like in the case of several phthalocyanine paints analysed in this paper). On the other hand, LIF [14,15] is based on the detection of the fluorescence emitted by molecules electronically excited with a coherent monochromatic laser source. Natural and synthetic pigments, organic and inorganic, may fluoresce due to the presence of delocalized electrons in molecules containing multiple aromatic rings, long chains of conjugated double bonds or di-azo bonds [16]. Since LIF results are not always unambiguous, the support of other spectroscopic methods may be necessary for a full material analysis.

Together with the above mentioned spectroscopic techniques, several other non-invasive optical methods and 3D imaging techniques have been applied to paintings in the past decades for the study of multi-layer internal structures, aiming at overcoming the detection limits imposed by the presence of highly scattering and semi-opaque materials [17–24]. Optical Coherence Tomography (OCT), originally developed for biological applications, provides high-resolution cross-sectional images of semi-transparent objects. It has proven to be effective for the in-depth visualization of low scattering varnish layers [17], enabling the distinction between aged and new varnishes [18]. In the presence of high-reflecting varnishes, the use of an OCT setup combined with confocal microscope optics may facilitate internal visualization, by focusing the beam inside the sample rather than on the outer varnish surface [19].

Non-linear optical microscopies (NLOM), working in various modalities, including Multi-Photon Excitation Fluorescence (MPEF) and Second and Third Harmonic Generation (SHG and THG), account for cutting-edge, non-invasive analysis based on non-linear optical processes, through which molecules simultaneously interact with two or more photons within the same quantum event. These non-linear optical phenomena can be observed when a given material is excited by a femtosecond (fs) pulsed laser, tightly-focused inside the medium by a high numerical aperture microscope objective. This ensures good penetration, of around 1 mm and high axial resolution in the range of micrometres. NLOM techniques [23,25–29] may provide 3D compositional and structural information based on the detection of fluorophores (by MPEF) [26], of crystalline or highly organized structures without inversion symmetry (by SHG) [27] or of local differences in refractive index and dispersion, i.e. interfaces, (by THG) [23]. NLOM analyses have been applied for 3D imaging of protective layers with the aim of supporting the removal of natural and synthetic varnishes during the cleaning. In-depth monitoring of morphological and chemical degradation of varnishes was carried out through the combination of MPEF and THG modalities in the case of aging[28] or laser ablation[29] processes. Cross-sections of pictorial layers were obtained through the NLOM modality of femtosecond pump-probe microscopy [30,31] and, more recently, MPEF imaging has been applied for the determination of thickness of egg-tempera paint layers [32]. A recent work has illustrated the complementary capabilities of OCT and NLOM for the study of painting materials [25] and has warned on the possibility of damaging non-transparent layers by irradiating them with the excessively high fluences of the femtosecond used in non-linear microscopies. Dal Fovo et al. [32] have examined tempera paint layers by MPEF upon femtosecond excitation at 740 nm and have showed that their thickness was underestimated due to the strong absorption and attenuation of the emitted fluorescence. Based on these antecedents, the main limitation of NLOM imaging seems to be associated with the presence of highly scattering and/or absorbing media (pigments), which obstruct the detection of the NLOM signal, and of the high laser fluences needed to excite a measurable non-linear optical signal.

As mentioned, the techniques applied in this work are particularly suitable for artworks diagnosis, due to their non-invasive character and in-situ applicability, which eliminates the necessity of sampling and moving the artwork [33]. Micro-Raman spectroscopy, FORS, LIF and OCT can be applied in-situ with portable and widely available systems. Latour et al. have demonstrated that NLOM can be applied directly to historic musical instruments using a setup able to collect nonlinear optical signals in the reflection mode [27].

In this work, we present the results obtained through the application of a set of non-invasive optical techniques for the chemical and physical characterization of six phthalocyanine acrylic paints (©Maimeri, Brera, IT): Primary Blue Cyan (PBC), Phthalo Blue (PB), Phthalo Green (PG), Cobalt Blue Hue (CBH), Permanent Blue Light (PBL) and Permanent Green Light (PGL). The optical behaviour and the chemical composition of the paints were investigated through a multi-analytical approach involving micro-Raman spectroscopy, FORS and LIF. This work also aims at further testing the applicability of advanced NLOM techniques at non-damaging laser excitation conditions, in probing painting materials with different light absorption properties. In-depth analyses were carried out non-

invasively by NLOM in the modality of MPEF in reflection mode, and the reliability of the results was assessed by comparison with OCT analysis.

2. Experimental

2.1. Materials

The set consists of six acrylic paints (Extra-fine acrylic colours, ©Maimeri Brera, IT) laid on glass coverslips ($2.5 \times 5\,cm^2$, 140 µm thickness). Three are pure Cu-Pc: Primary Blue Cyan (PBC), PB15:3 – 74160; Phthalo Blue (PB), PB15:1 – 74160 and Phthalo Green (PG), PG7 – 74260. The remaining three are mixtures of Cu-Pc and different organic compounds, like aniline and acetoacetanilide, and inorganic titanium dioxide: Cobalt Blue Hue (CBH), PB15:3 – 74,160, PW6 – 77891, PB29 – 77007; Permanent Blue Light (PBL), PB15:3 – 74,160, PG7 – 74260, PW6 – 7789 and Permanent Green Light (PGL), PG7 – 74260, PW6 – 77891, PY97 – 11767. Each pigment is referenced with two indexes, namely the generic name (GN) and constitution number (CN), according to the globally recognized Colour Index Database [3]. Colour indexes are descriptors used for pigments classification, to facilitate their identification in the industrial/commercial field. These indexes are not directly connected to CIEL*a*b* values, which instead are colorimetric parameters, experimentally measured and reported in this work for a further characterization of the paints. CIEL*a*b* coordinates, measured through Fibre Optics Reflectance Spectroscopy (FORS) (see Section 2.2.2), are reported in Fig. 2. Bright-field images and micro-images, obtained with a Leica DFC 420 charge-coupled detector (CCD) camera, are also shown in this Figure.

2.2. Methods

2.2.1. Micro-Raman Spectroscopy

Raman spectra were collected using a Ranishaw InVia 0310–02 System based on a continuous Nd:YAG laser excitation source at 532 nm. The diameter of the laser spot on the sample was diffraction limited to 1 µm by the objective lens (50×). The system is equipped with a Leica microscope and an electrically refrigerated CCD camera. The wavenumber resolution was $4\,cm^{-1}$ and the acquisition time set for measurements of 10 s. Low laser powers (0.15–0.3 mW) were used to prevent degradation of the samples [8].

2.2.2. Fibre Optics Reflectance Spectroscopy (FORS)

FORS spectra were acquired with a Zeiss Multi-Channel Spectrometer, including a MCS 521 VIS NIR-extended module and a MCS 511 NIR 1.7 module with spectral sensitivity in the 304–1100 nm and 950–1700 nm ranges, with spectral resolution of 3.2 nm and 6.0 nm, in the visible and IR region, respectively. The illumination/observation geometry is 45°/0°. For measurements, each sample was placed on a 100% reflecting background (Spectralon) and each spectrum was the resulting average of three acquisitions from each of three measurements points that were selected for each sample. The output signal was processed through a dedicated software, providing also CIEL*a*b* coordinates [34–36], computed using the measured Vis spectrum with standard D65 illuminant and 2° observer (Fig. 2).

2.2.3. Laser Induced Fluorescence (LIF)

Excitation of the fluorescence emission was induced by a Q-switched Nd:YAG laser operating at its 4th harmonic at 266 nm, with pulse duration of 15 ns, and repetition rate of 1 Hz. As in the case of micro-Raman analyses (see Section 2.2.1.), the laser pulse energy was very low, of the order of 0.5 mJ, to avoid degradation of samples during measurements. The luminous emission was collected and dispersed by a 0.30 m spectrograph with a 300 lines/mm grating (TMc300, Bentham) coupled to an intensified charged coupled device (CCD, 2151 Andor Technologies). The temporal gate (width of 3 µs) was fixed at zero time delay with respect to the arrival of the laser pulse to the surface of the sample.

2.2.4. Optical Coherence Tomography (OCT)

In-depth imaging was performed with a Time-Domain confocal OCT prototype developed at Istituto Nazionale di Ottica (CNR-INO, Italy), which combines confocal microscope optics with the OCT setup. The system operates at a wavelength of 1550 nm with an axial resolution of 10 µm in air and a lateral resolution of 2.5 µm. The maximum acquisition length is 25 mm, both in the x and y directions, whereas the in-depth probing length is 1 mm.

2.2.5. Multi-Photon Excitation Fluorescence (MPEF)

In-depth analysis was also performed with a non-linear optical microscope developed at Instituto de Química Física Rocasolano (IQFR-CSIC, Spain) that allows the collection of the MPEF signals from the focal volume at the sample plane in the reflection mode, as depicted in Fig. 3. The excitation light source is a mode-locked Ti:Sapphire femtosecond laser emitting at 800 nm, with average power of 680 mW, delivering 70 fs pulses at a repetition rate of

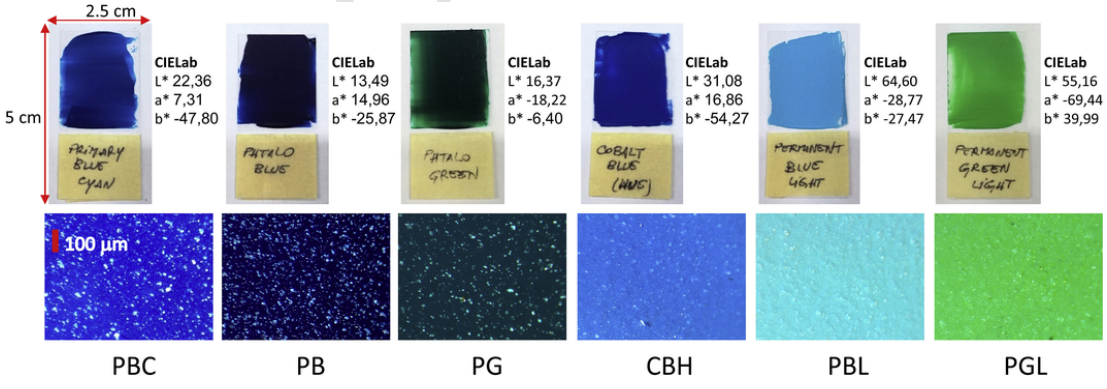

Fig. 2. Copper phthalocyanine paint layers applied on glass coverslips (upper row) and micro-images (lower row, $740 \times 550\,\mu m^2$) showing paint micromorphology. CIEL*a*b* values as measured through FORS analysis, are also reported (see text).

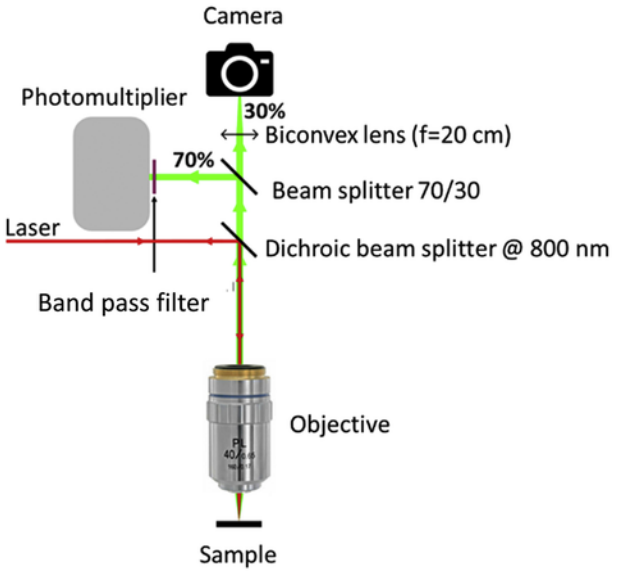

Fig. 3. Layout of the non-linear optical microscope used for MPEF measurements.

80 MHz. A variable neutral density filter (NDC-50C-2M, Thorlabs) was used to control the laser power reaching the sample. For the present measurements, the average power was in the range of 1–15 mW, values far from the damage threshold of the paints (as monitored through CCD online visualization of the sample surface during the femtosecond laser excitation). The laser beam was conducted to the sample through the aperture of a microscope objective lens (M Plan Apo HL 50×, Mitutoyo, NA 0.42) by using a dichroic beam splitter (FF750-SDi02-25 × 36, Semrock) with high reflection at 800 nm.

The laser focal plane was selected with motorized translation XYZ stages (Standa 8MVT100–25-1 for XY and Standa 8MTF for Z). The lateral and in-depth resolutions achieved are of 1 and 2 μm, respectively. A LabVIEW interface was used to control both scanning and data acquisition procedures. The MPEF signals were collected in the backward direction through the microscope objective lens and a beam splitter (70/30) and measured using a photomultiplier tube (9783B, ET Enterprises) connected to a lock-in amplifier (SR810 DSP, Stanford Research Systems) to ensure high amplification and signal-to-noise ratio. A short pass filter (335–610 nm, Thorlabs FGB37S) was placed at the entrance of the photomultiplier to cut off the reflected laser light. The remaining 30% of the MPEF signal was sent to a CCD camera (Thorlabs DCC1645C) for online visualization of the sample surface and the signal collection process.

Table 1
Main Raman bands of six analysed copper phthalocyanine paints.

Paint (acronym)	Main Raman bands [cm^{-1}] and relative intensity[a], λ_{exc} = 532 nm
Primary Blue Cyan (PBC)	231w, 255w, 590 m, 680 m, 747w, 951w, 1037w, 1137w, 1341w, 1451 m, 1527s, 1595w, 2672w, 2870w, 2976w, 3056w
Phthalo Blue (PB)	
Phthalo Green (PG)	142w, 162w, 505 m, 685 s, 818w, 978w, 1080 m, 1200w, 1284 m, 1340w, 1388 m, 1503s, 1536s
Cobalt Blue Hue (CBH)	230 m, 260 m, 548 s, 583 m, 680 m, 747w, 808w, 951w, 1096 m, 1145w, 1450 m, 1530s, 1584w, 1644w, 2192w
Permanent Blue Light (PBL)	143w, 231 m, 255 m, 450 s, 590 s, 609 s, 680 s, 747w, 831w, 951w, 1008w, 1037w, 1137 m, 1341s, 1451s, 1527s, 1595w, 2870w, 3056w
Permanent Green Light (PGL)	153w, 309 m, 505w, 615w, 685 s, 818w, 978w, 998w, 1008w, 1080 m, 1200 m, 1284s, 1332w, 1340 m, 1388s, 1455w, 1503s, 1536s, 1591w, 1668w

[a] s: strong; m: medium; w: weak.

3. Results and Discussion

3.1. Micro-Raman Spectroscopy

The chemical composition of the six analysed paints was determined through comparison with spectral information reported in literature and databases available online [37–39]. The main Raman bands assigned for each Cu-Pc pigment, together with their respective intensities, are reported in Table 1, while the chemical compositions are summarized in Table 2. As an example, Fig. 4 includes the Raman spectra acquired in the PB and PBL samples.

Spectra of PBC and PB display numerous common bands (the most intense ones are centred at about 590, 680, 1451 and 1527 cm^{-1}), hampering the distinction between the two pigments.

Table 2
Chemical composition of the six analysed copper phthalocyanine paints.

	PB15:1 Inorganic Copper Phthalocyanine α [$C_{32}H_{16}CuN_8$]	PB15:3 Inorganic Copper Phthalocyanine β [$C_{32}H_{16}CuN_8$]	PG7 Organic Chlorinated Phthalocyanine [$C_{32}H_3Cl_{13}CuN_8$ to $C_{32}HCl_{15}CuN$]	PB29 Inorganic Ultramarine Sodium Polysulphide-Aluminosilicate	PY97 Organic Arylide yellow [azo coupling of aniline and acetoacetanilide]	PW6 Inorganic Titanium Dioxide [TiO_2]
Primary Blue Cyan (PBC)		✓				(traces)
Phthalo Blue (PB)	✓					
Phthalo Green (PG)			✓			
Cobalt Blue Hue (CBH)		✓		✓		✓
Permanent Blue Light (PBL)		✓	✓			✓
Permanent Green Light (PGL)			✓		✓	

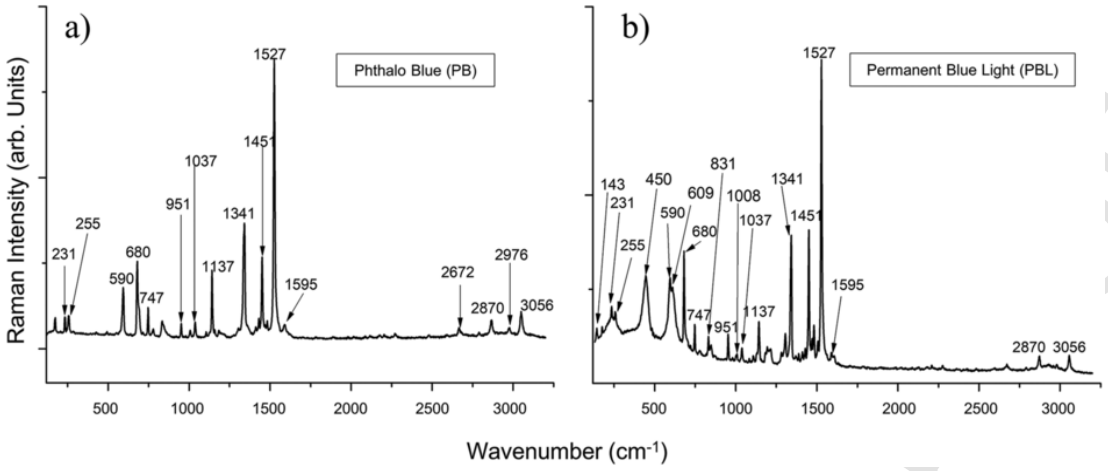

Fig. 4. Micro-Raman spectra of a) Phthalo Blue (PB) and b) Permanent Blue Light (PBL) acrylic paints upon excitation at 532 nm. (For interpretation of the references to colour in this figure legend, the reader is referred to the web version of this article.)

Concerning PG, the most significant bands appear at 685, 1503 and 1536 cm^{-1}. Raman analysis on these three pure phthalocyanine pigments (PB, PBC, PG) allowed assignment of the bands in accordance with literature [7].

The three mixtures (CBH, PBL and PGL) and the PBC paints show bands ascribed to additional components. The bands at 1332, 1455, 1591 and 1668, cm^{-1} in the PGL spectrum correspond to the pigment Arylide Yellow, PY97 [40]. Bands at 260, 548, 583, 808, 1096, 1644 and 2192 cm^{-1} in the CBH spectrum allow identifying the presence of Ultramarine, PB29. Bands at 143, 231, 450, 609 cm^{-1} in PBL, CBH, and PBC (traces) are due to Titanium White, PW6, in rutile form. We found some discrepancies with the composition declared by the manufacturer. The most significant one concerns PGL paint, in which bands of barium sulphate (at 998 cm^{-1}) and calcium sulphate (at 1008 cm^{-1}) where observed, their presence possibly related to a component added as filler. Also in this case, bands assigned to the Cadmium Yellow pigment (at 153, 309, 615 cm^{-1}) were detected [41]. Furthermore, no traces of titanium dioxide were found in PGL, in contrast with what was reported by the manufacturer.

3.2. Fibre Optics Reflectance Spectroscopy (FORS)

The reflectance spectra of the six acrylic paints studied in this work are reported in Fig. 5a, b, c, showing specific spectral zones for better differentiation of the paint materials. Previous studies [42] have shown that Cu-Pc pigments present specific spectral features, which upon combined analysis by Raman spectroscopy allow discriminating between different compounds. It is observed that all the analysed paints display varying degrees of transparency at 800 nm, which is the wavelength of the femtosecond laser used for MPEF measurements, and in the spectral region between 335 and 610 nm, where the induced multiphoton emission can be detected. This variation is important in view of the NLOM measurements performed on the samples, as it provides a range of conditions to test the capacity of thickness determination by this technique.

Fig. 5b displays the second derivative of the reflectance function for Primary Blue Cyan, Phthalo Blue and Phthalo Green paints in the NIR region between 700 and 900 nm. A possible differentiation between the three paint is based on the identification of the inflection points, which are located at 800, 860 and 900 nm for PBC, PB and PG respectively. Fig. 5c shows the spectra of all Cu-Pc paints in the 350–700 nm region. Further confirmation of the chemical composition of these paints is based on the detection of a shoulder at 410 nm attributed to titanium dioxide in rutile form [42].

3.3. Laser Induced Fluorescence (LIF)

LIF spectra of the six Cu-Pc paints are displayed in Fig. 6. The common broad emission band between 280 and 380 nm is attributed to the acrylic binder, in consistency with previous published studies [13,43,44]. The emission bands at higher wavelengths, between 380 and 580 nm, are characteristic of each pigment. Specifically, CBH and PBC show very similar fluorescence emissions, with maxima at 400 and 440 nm, PBL and PB display a broad, somewhat structured emission band centred at around 400 nm, and PG emits a relatively less intense fluorescence band located between 380 and 550 nm. The emissions of these five paints are associated with characteristic fluorescence emission bands of phthalocyanines [43]. PGL shows a band slightly shifted towards longer wavelengths (460–570 nm, centred at 500 nm) with respect to the other pigments, which is associated with azo compounds emission [43].

The spectra presented in Fig. 6 have not been corrected by absorption of the pigments or the acrylic dispersion medium and, therefore, the intensity of the emission of each paint should reflect the effect of the absorption coefficient and of the fluorescence quantum yield of the phthalocyanines. However, as regarding the NLOM measurements performed here, the identification of the LIF emission bands collected by excitation at 266 nm, as described above, is necessary to ensure the proper detection of the MPEF signals. Given the wavelength of the femtosecond laser source, it is expected that three-photon absorption at 800 nm would yield similar fluorescence spectra than those collected by one-photon absorption at 266 nm. The detection range of the non-linear optical microscope is limited by the filter in front of the photomultiplier to the region of 335–610 nm. According with LIF measurements, this implies that MPEF signals include emission from the binder and pigment components of the paints.

3.4. Optical Coherence Tomography (OCT)

For each sample, two OCT profiles were acquired along two perpendicular lines in the middle of the painted surface and indicated in Fig. 7a. The real thicknesses of the paint layers were evaluated as an average of six values measured along a 1 mm OCT profile, taking into account the refractive index of the medium ($n = 1.5$) [45]. The

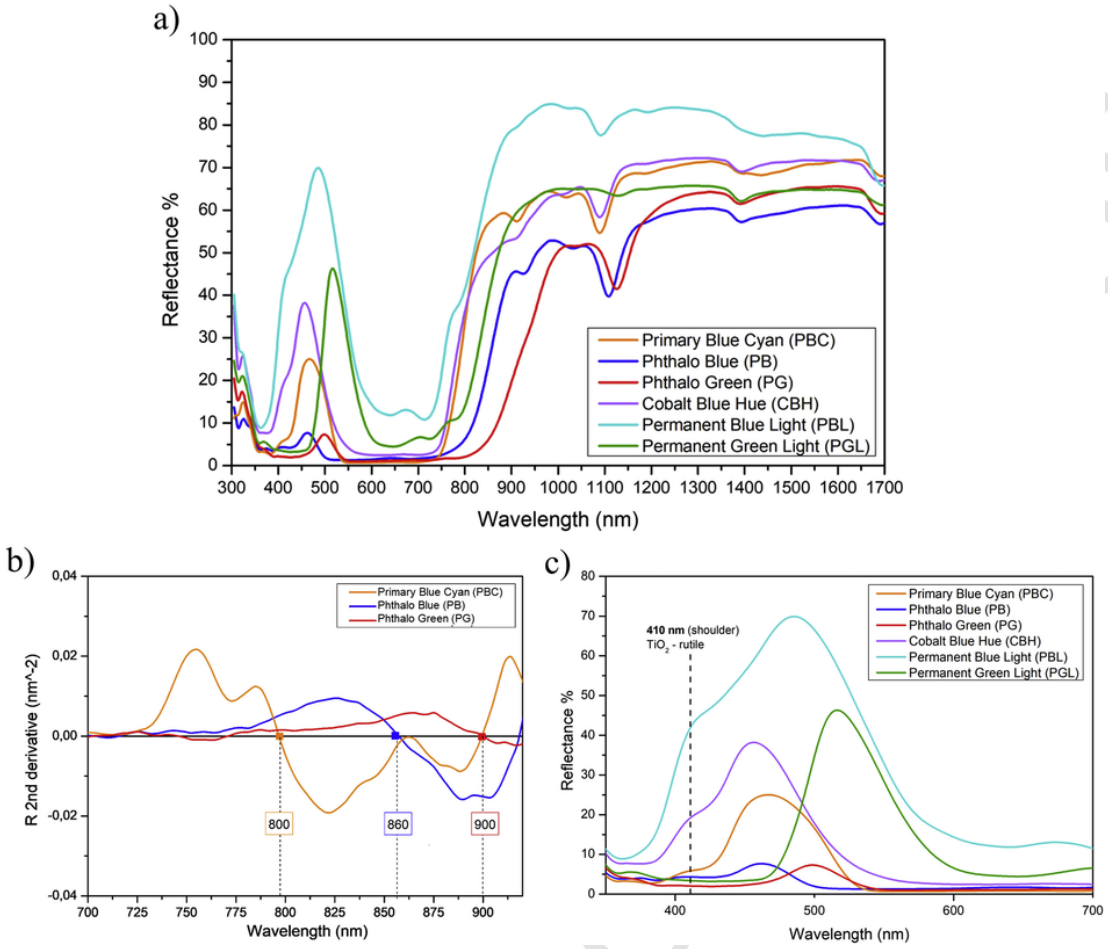

Fig. 5. Reflectance spectra of Cu-Pc paints: a) in the 300–1700 nm spectral range; b) second derivative curves for PBC, PB and PG in the 700–920 nm range, where the zeros of the functions correspond to the position of the inflection points; c) zoom out of the reflectance spectra of Cu-Pc paints in the 350–700 nm. The shoulder at 410 nm highlights the presence of TiO_2 only in PBC, CBH and PBL paints.

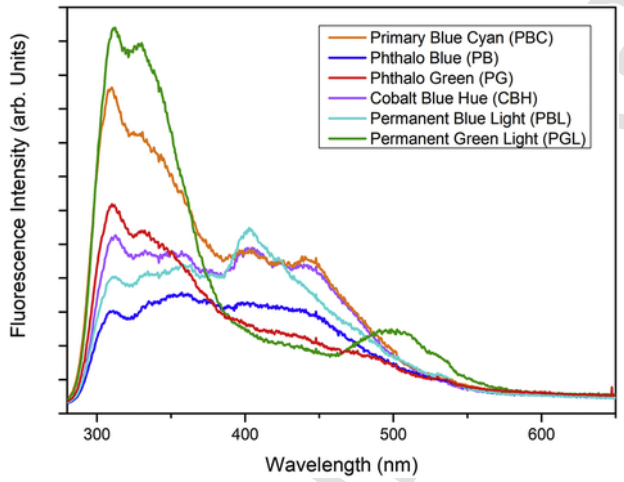

Fig. 6. LIF spectra acquired by excitation at 266 nm of the Cu-Pc pigments.

signal coming from the glass support was taken as a reference, assuming that 1 pixel corresponds to 1 µm along the in-depth direction and to 5 µm along the scanning direction of the tomographic image.

It is worth mentioning that the acquired OCT profiles, as the ones shown for Primary Blue Cyan sample in Fig. 7, enable the visualization of the lower glass/air interface due to the transparency of the Cu-Pc paints at the wavelength of the OCT source of 1550 nm. Differently, no distinction between paint and glass is possible, due to the negligible difference in refractive index between the two materials. For that reason, the thickness of the paint layers is assessed taking as reference the glass surface visible at the border of each sample. Table 3 displays the thickness values determined by OCT for the samples of this study.

3.5. Multi Photon Excitation Fluorescence (MPEF)

MPEF signals were collected for all the six Cu-Pc paints in an area of $5 \times 5\,mm^2$ approximately located in the middle of each sample, in order to ensure a correct comparison with the OCT tomograms. On the basis of signal intensity, the detection was optimized in each case by setting the laser power to the most suitable range, although it never exceeded 15 mW to ensure non-damaging measuring conditions [25]. The dependence of the MPEF signal with the depth below the surface of the paint (*Z*-scan) was measured at five different sample positions of the analysed area. MPEF profiles were normalized and fitted with a Lorentzian function, and the full width at half maximum (FWHM) was taken as an estimation of the paint layer apparent thickness. To obtain the real thickness, the FWHM values where subsequently corrected by applying the apparent depth correction factor (*F*), according to the formula[46]

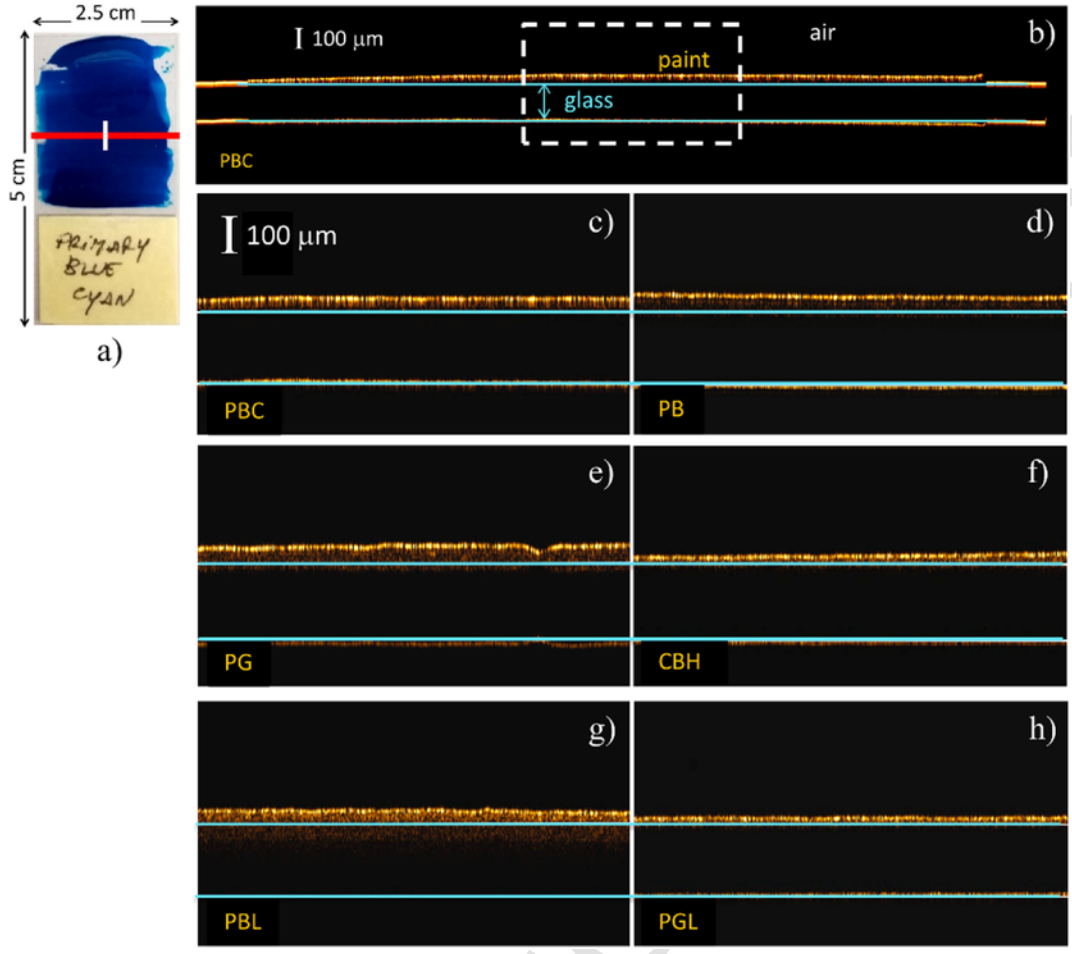

Fig. 7. a) Bright field image of the Primary Blue Cyan sample showing the position of the two OCT profiles acquired on each sample: red line (25 mm scanning length and 1 mm deep) and white line (5 mm scanning length and 1 mm deep), orthogonally oriented and crossing at the centre of the painted surface; b) OCT tomogram of PBC paint acquired along the red line (25 × 1 mm; scale bar = 100 µm in-depth) displaying the paint layer (coloured in yellow) over the glass support (light-blue lines); the central area, considered for paint thickness evaluation, is highlighted by the dotted-line rectangle; c)–h) tomograms of the central area for the six phthalocyanine paints. (For interpretation of the references to colour in this figure legend, the reader is referred to the web version of this article.)

Table 3
Comparison between thicknesses measured by MPEF and OCT.

Sample	$FWHM^{corr}$ [µm] ± st. error	OCT thickness [µm] ± st. dev.
PBC	53 ± 2	46 ± 3
PB	53 ± 3	48 ± 3
PG	50 ± 4	51 ± 2
CBH	30 ± 2	28 ± 3
PBL	40 ± 1	38 ± 2
PGL	25 ± 1	22 ± 2

$$F = \frac{1 - \sqrt{1 - NA^2}}{n - \sqrt{n^2 - NA^2}} = 1.54$$

where n is the refractive index of the sample (1.5), computed following ref. [40], and NA the effective numerical aperture of the focusing objective lens (0.42). The collected MPEF signals as a function of depth are represented in Fig. 8, together with Lorentzian function fits. Although in this figure, the signals are normalized to their maximum value, it should be noticed that their magnitude varies with the degree of transparency at 800 nm (as depicted in Fig. 5). As an example, the MPEF signal from the highly absorbing PG and PB paints is around one order of magnitude lower than the signal measured in the rest of paints. The thickness of the paint layers after correction ($FWHM^{corr}$) are reported in Table 3 with standard errors and OCT measured thickness for comparison.

Table 3 brings evidence of the good agreement between the paint thickness values determined in this work through MPFE and OCT despite the varying degree of transparency of the samples at the femtosecond laser excitation wavelength. As it has been mentioned above, measurements were performed at low laser fluence levels which resulted in weak MPEF signal for some of the highly absorbing samples, like PG and PB. Despite these stringent measuring conditions, the signal-to-noise ratio was high enough to determine the thickness of the layer, thus allowing the comparison with OCT results. Notwithstanding the usefulness of the THG modality of NLOM to determine the layer boundaries, the results shown herein demonstrate that the proper choice of laser excitation wavelength and average power and of the spectral range for collection of the fluorescence signals is crucial to ensure a correct estimation of thickness paint layers by MPEF.

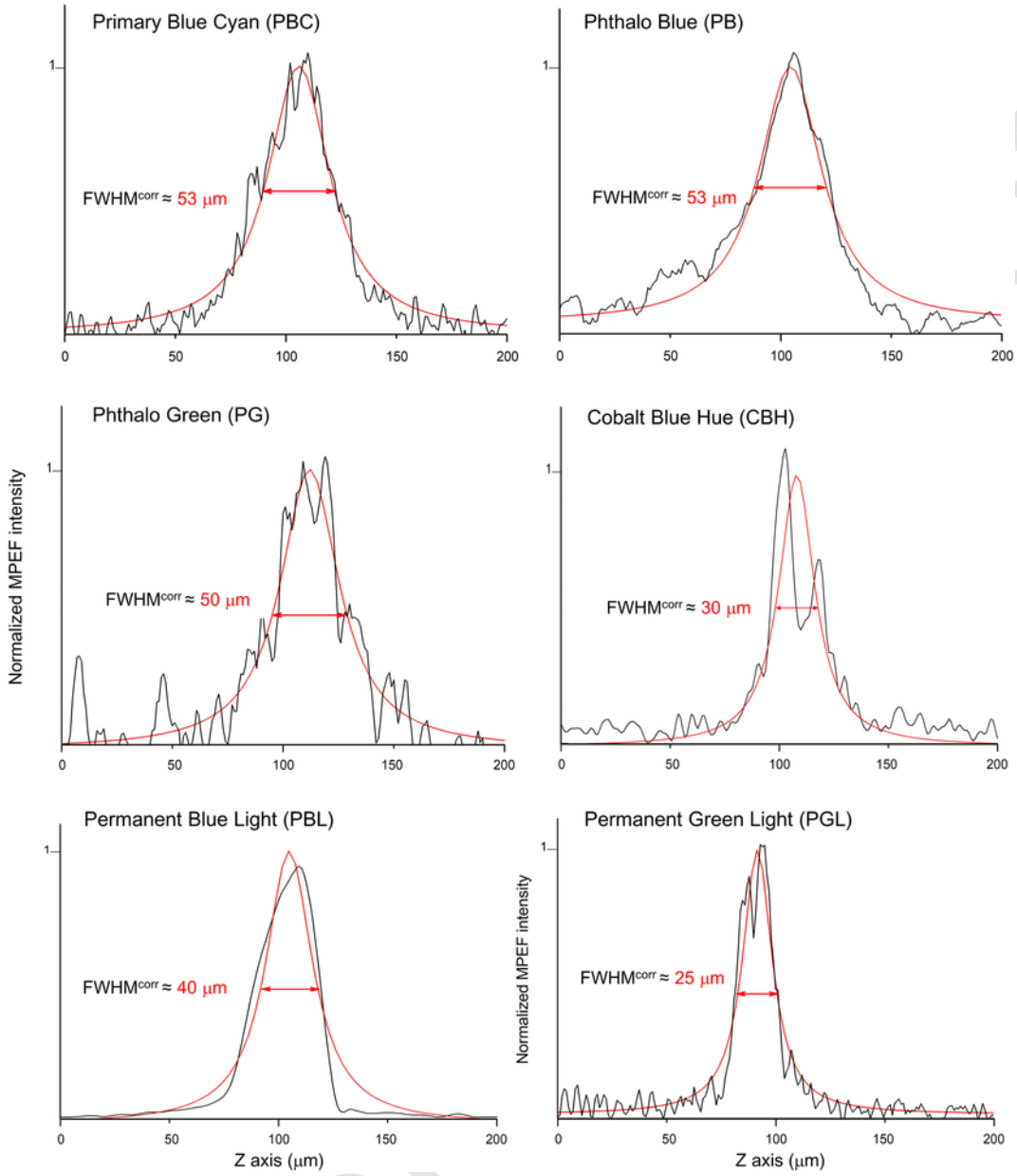

Fig. 8. *Z*-Scans of the MPEF signals of Cu-Pc paint samples (in black) and fits by a Lorentzian function (in red). The corresponding FWHM values after refractive index corrections are indicated in red. (For interpretation of the references to colour in this figure legend, the reader is referred to the web version of this article.)

4. Conclusions

This paper describes the characterization of a set of purposely developed samples of six phthalocyanine acrylic paints using non-invasive spectroscopic, interferometric and non-linear optical microscopy techniques. Chemical-physical characterization of the paint materials was obtained by laser micro-Raman spectroscopy and Fibre Optics Reflectance Spectroscopy (FORS), which provided complementary information for the identification of molecular compounds in each paint and for highlighting in some cases discrepancies with the chemical composition declared by the manufacturer. The application of these two techniques made also possible to differentiate between the two pure phthalocyanine Phtalo Blue and Primary Blue Cyan (PB15:1 and PB15:3 pigments, α- and β- polymorphic forms, respectively), having very similar composition but different reflectance behaviour. The measurement of the laser induced fluorescence (LIF) spectra of the paints upon excitation at 266 nm allowed for discriminating the bands emitted by the acrylic binder from those of the pigments, while non-invasive stratigraphic analysis by optical coherence tomography (OCT) yielded an estimation of the paint thicknesses. The results obtained using these techniques served to select the adequate excitation and signal collection conditions for studying the phthalocyanine acrylic paints by the cutting-edge Multi-Photon Excitation Fluorescence (MPEF) technique, a modality of non-linear optical microscopy (NLOM) seldom applied on painting materials. Upon femtosecond laser excitation at 800 nm, and applying average powers far below the paint damage thresholds, it was possible to determine the paint layers' thickness through this technique. The good agreement between the thickness values estimated with OCT and MPEF

serve to validate the latter technique for paint materials that display sufficient degree of transparency to the excitation laser wavelength and in the spectral range of the emitted fluorescence. The NLOM measurements described here were carried out in the reflection mode, thus providing the possibility to apply these techniques to coatings of painting materials laying on an opaque substrate (board, wood, canvas, etc.) for in-situ studies. Further research is in progress on samples simulating the real structure of a painting, and by combining MPFE with other modalities of NLOM such as Second and Third Harmonic Generation (SHG and THG).

Conflicts of Interest

There are no conflicts to declare.

Uncited reference

[46]

Acknowledgements

The research leading to these results was funded by the EU Community's H2020 Research Infrastructure program under the IPERION CH Project (GA 654028) and by Ministerio de Economía, Industria y Competitividad (MINECO) of Spain under Project CTQ2016-75880-P.

References

[1] N. Sonoda, Stud. Conserv. 44 (3) (1999) 195–208, https://doi.org/10.1179/sic.1999.44.3.195.
[2] R.P. Linstead, J. Chem. Soc. 212 (1934) 1016–1017, https://doi.org/10.1039/JR9340001016.
[3] R.P. Linstead, A.R. Lowe, J. Chem. Soc. 214 (1934) 1022–1027, https://doi.org/10.1039/JR9340001022.
[4] https://colour-index.com, Accessed February 2018.
[5] N. Khandekar, C. Mancusi-Ungaro, H. Cooper, C. Rosenberger, K. Eremin, K. Smith, J. Stenger, D. Kirby, Stud. Conserv. 55 (2010) 204–215.
[6] C. Defeyt, D. Struvay, e-Preservation Science (e-PS), vol. 11, 20146–14, (ISSN: 1581-9280 web edition).
[7] C. Defeyt, P. Vandenabeele, B. Gilbert, J. Van Pevenage, R. Clootse, D. Strivaya, J. Raman Spectrosc. 43 (2012) 1772–1780, https://doi.org/10.1002/jrs.4125.
[8] C. Defeyt, P. Walter, H. Rousseliére, P. Vandenabeele, B. Vekemans, L. Saiman, D. Strivay, Stud. Conserv. 63 (2017) 24–35.
[9] F. H. Moser and A. L. Thomas, 1964, 41(5), 245, doi:https://doi.org/10.1021/ed041p245.
[10] F.M. Smith, J.D. Easton, J. Oil Col. Chem. Assoc. 49 (1966) 614–630.
[11] H. Edwards, J.M. Chalmers, RSC Analytical Spectroscopy Series, The Royal Society of Chemistry, London, 2005.
[12] E. Cloutis, L. Norman, M. Cuddy, P. Mann, J. Near Infrared Spectrosc. 24 (2016) 119–140.
[13] M. Marinelli, A. Pasqualucci, M. Romani, G. Verona-Rinati, J. Cult, Heritage 23 (2017) 98–105, https://doi.org/10.1016/j.culher.2016.09.005.
[14] R. de la Rie, E. Fluorescence of paint and varnish layers (Part I, II, III), Stud. Conserv. 27 (1–7) (1982) 65–69, (102–108).
[15] D. Anglos, M. Solomidou, I. Zergioti, V. Zafiropulos, T. Papazoglou, C. Fotakis, Appl. Spectrosc. 50 (1996) 1331–1334.
[16] A. Nevin, G. Spoto, D. Anglos, Appl. Phys. A Mater. Sci. Process. 106 (2012) 339–361, https://doi.org/10.1007/s00339-011-6699-z.
[17] P. Targowski, M. Gòra, M. Wojtkowski, Hindawi Publishing Corporation, Laser Chem., (2006), 35373, 11 pages https://doi.org/10.1155/2006/35373.
[18] H. Liang, M. Cid, R. Cucu, G. Dobre, A. Podoleanu, J. Pedro, D. Saunders, Opt. Express 13 (2005) 6133–6144.
[19] R. Fontana, A. Dal Fovo, J. Striova, L. Pezzati, E. Pampaloni, M. Raffaelli, M. Barucci, Appl. Phys. A Mater. Sci. Process. 121 (3) (2015) 957–966, https://doi.org/10.1007/s00339-015-9505-5.
[20] B. Blümich, J. Perlo, F. Casanova, Prog. Nucl. Magn. Reson. Spectrosc. 52 (2008) 197.
[21] N. Proietti, D. Capitani, V. Di Tullio, Sensors 14 (4) (2014) 6977.
[22] F. Presciutti, J. Perlo, F. Casanova, S. Glöggler, C. Miliani, Appl. Phys. Lett. 93 (2008), 033505.
[23] G. Filippidis, M. Massaouti, A. Selimis, E.J. Gualda, J.M. Manceau, S. Tzortzakis, Appl. Phys. A Mater. Sci. Process. 106 (2) (2012) 257–263, https://doi.org/10.1007/s00339-011-6691-7.
[24] A.J.L. Adam, P.C.M. Planken, S. Meloni, J. Dik, Opt. Express 17 (5) (2009) 3407.
[25] H. Liang, M. Mari, C.S. Cheung, S. Kogou, P. Johnson, G. Filippidis, Opt. Express 25 (2017) 19640–19653.
[26] G. Filippidis, G.J. Tserevelakis, A. Selimis, C. Fotakis, Appl. Phys. A Mater. Sci. Process. 118 (2015) 417–423, https://doi.org/10.1007/s00339-014-8357-8.
[27] G. Latour, J.P. Echard, M. Didier, M.C. Schanne-Klein, Opt. Express 20 (2012) 24623–24635, https://doi.org/10.1364/OE.20.024623.
[28] G. Filippidis, M. Mari, L. Kelegkouri, A. Philippidis, A. Selimis, K. Melessanaki, M. Sygletou, C. Fotakis, Microsc. Microanal. 21 (2015) 510–517, https://doi.org/10.1017/S1431927614013580.
[29] M. Oujja, S. Psilodimitrakopoulos, E. Carrasco, M. Sanz, A. Philippidis, A. Selimis, P. Pouli, G. Filippidis, M. Castillejo, Phys. Chem. Chem. Phys. 19 (2017) 22836, https://doi.org/10.1039/c7cp02509b.
[30] T.E. Villafana, W.P. Brown, J.K. Delaney, M. Palmer, W.S. Warren, M.C. Fischer, Proc. Natl. Acad. Sci. U. S. A. 111 (2014) 1708–1713, https://doi.org/10.1073/pnas.1317230111.
[31] T.E. Villafana, W. Brown, W.S. Warren, M. Fischer, Proc. SPIE 9527 (2015) 9, https://doi.org/10.1117/12.2184758.
[32] A. Dal Fovo, R. Fontana, J. Striova, E. Pampaloni, M. Barucci, M. Raffaelli, R. Mercatelli, L. Pezzati, R. Cicchi, Lasers in the conservation of artworks XI, in: P. Targowski, et al. (Eds.), Proceedings of LACONA XI, NCU Press Torun, 2017https://doi.org/10.12775/3875-4.10.
[33] M. Melo, A. Nevin, P. Baglioni, Pure Appl. Chem. 90 (2018) 429–433, IUPAC Journal https://doi.org/10.1515/pac-2018-0106.
[34] R.G. Kuehni, Color: An Introduction to Practice and Principles, Wiley, New York, USA, 1997.
[35] R.G. Kuehni, Color Space, and its Division, Wiley, New York, USA, 2003.
[36] CIE, CIE44: 1979, In: Absolute Methods for Reflection Measurements, 1974.
[37] L. Burgio, R. Clark, Spectrochim. Acta A 57 (2001) 1491–1521.
[38] M.C. Caggiani, A. Cosentino, A. Mangone, Microchem. J. 129 (2016) 123–132, (doi:10.1016).
[39] N. Marchettini, A. Atrei, F. Benetti, N. Proietti, V. Di Tullio, M. Mascalchi, I. Osticioli, S. Siano, I. Turbanti Memmi, 2013, 29, 2, 153–159, doi https://doi.org/10.1179/1743294412Y.0000000065.
[40] C.S. Nadim, S. Zumbuehl, F. Delavy, A. Fritsch, R. Kuehnen, Spectrochim. Acta A 73 (2009) 505–524, https://doi.org/10.1016/j.saa.2008.11.029.
[41] B.W. Singer, D.J. Gardiner, J.P. Derow, The Paper Conservator, vol. 19, 1995https://doi.org/10.1080/03094227.1993.9638401, (published online 2010).
[42] G. Poldi, S. Caglio, Opt. Spectrosc. 114 (2013) 929–935.
[43] M. Romani, F. Colao, R. Fantoni, M. Guiso, M.L. Santarelli, J. Appl. Las. Spectrosc. 1 (2014) 29–36.
[44] R. Fantoni, L. Caneve, F. Colao, L. Fiorani, A. Palucci, R. Dell'Erba, V. Fassina, J. Cult. Herit. 14S (2013) S59–S65, https://doi.org/10.1016/j.culher.2012.10.025.
[45] S. Lawman, H. Liang, Appl. Opt. 50 (32) (2011), (0003-6935/11/326039).
[46] G.W. White, Microscope 18 (1970) 51–59.